Computers & Structures Vol. 30, No. 1/2, pp. 269–274, 1988
Printed in Great Britain.

0045-7949/88 $3.00 + .00

A SOLID ELEMENT FORMULATION FOR LARGE DEFLECTION ANALYSIS OF COMPOSITE SHELL STRUCTURES

Y. H. KIM and S. W. LEE
Department of Aerospace Engineering, University of Maryland, College Park, MD 20742, U.S.A.

Abstract—An 18-node solid element has been developed to model the behavior of laminated composite shells undergoing large deflection. The element formulation utilizes independently assumed strain in addition to assumed displacement. The strain and the determinant of the Jacobian matrix are assumed to be linear in the thickness direction. This allows analytical integration through the thickness regardless of ply layups. Numerical results demonstrate the validity of the present formulation.

1. INTRODUCTION

Laminate composite structures have become increasingly popular in many engineering fields. This is due to the high specific stiffness and the high specific strength of composite structures. However, the intelligent use of composite structures requires a reliable analysis technique such as the finite element method.

During the last decade or so, a number of finite element approaches have been proposed for the analysis of composite shell structures[1–5]. Among these, [5] develops a nine-node composite shell element based on the degenerate solid shell concept and the hybrid/mixed formulation with assumed independent strain[6]. The formulation in [5] allows modelling of geometrically nonlinear composite shells. Recently, a new formulation has been proposed[7], in which the lower order assumed strain part is substituted with the strain from the assumed displacement field.

As an alternate approach, a three dimensional, 18-node solid element was developed for analysis of thin shell structures[8]. In [8], a new mixed formulation is used for the finite element modelling. In addition, a modified stress–strain relation is used to represent thin shell behavior by decoupling inplane and normal strain. As far as the description of geometry and kinematics of deformation are concerned, the three dimensional solid element formulation is the simplest among all approaches. Numerical tests conducted in [8] show that the three dimensional solid element formulation can provide a reliable finite element model free of locking while kinematically stable. However, the scope of the study in [8] was limited to a small displacement and isotropic elastic material. The formulation used in [8] is extended to large deflection in [9] in which the conventional mixed formulation is used instead of the new mixed formulation.

In the present paper, the solid element formulation is extended to model geometrically nonlinear composite shells. The strain and the determinant of the Jacobian matrix are assumed to be linear in the thickness direction to allow analytical integration regardless of ply layups. Formation of the stiffness matrix, selection of assumed strain, the modified stress–strain relation and numerical examples are discussed in the following sections.

2. FORMULATION

Figure 1 shows an 18-node solid element in three dimensional space. For convenience, a local orthogonal coordinate system is defined at a generic point as well as the global Cartesian coordinate system. The global coordinate system has components X, Y and Z and the local coordinate system has components x, y and z along the direction of unit vectors $\mathbf{a}_1$, $\mathbf{a}_2$ and $\mathbf{a}_3$. In addition to the global coordinate system and the local coordinate system, the parent coordinate system with components ξ, η and ζ is used to describe the shape functions. The local coordinate system is chosen such that unit vectors $\mathbf{a}_1$ and $\mathbf{a}_2$ are tangent to the ξ–η plane and $\mathbf{a}_3$ is orthogonal to $\mathbf{a}_1$ and $\mathbf{a}_2$. The detail description of the local coordinate system is given in [9].

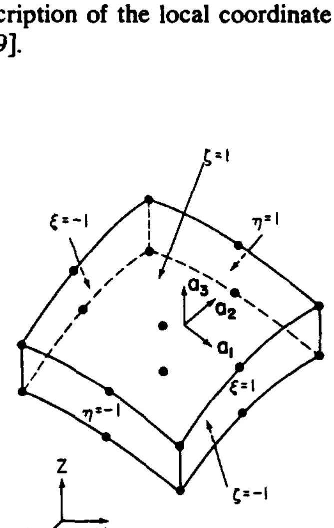

Fig. 1. Eighteen-node solid element.

Tangent stiffness matrix and load vector

For a solid body in equilibrium

$$\int (\delta\bar{\mathbf{E}}^L)^T \mathbf{S}^L \,\mathrm{d}v - \delta W = 0, \qquad (1)$$

where $\mathbf{S}^L$ is the second Piola–Kirchhoff stress vector, $\delta\bar{\mathbf{E}}^L$ is the virtual strain vector, δW is the external virtual work, and superscript T stands for the transpose. The variables with superscript L are defined with respect to the local coordinate system, and the integration is defined over the volume v in the undeformed configuration.

Introducing an independent strain vector $\mathbf{E}^L$ in addition to the displacement-dependent strain vector $\bar{\mathbf{E}}^L$, the compatibility condition is expressed as

$$\int (\delta\mathbf{S}^L)^T (\bar{\mathbf{E}}^L - \mathbf{E}^L)\,\mathrm{d}v = 0, \qquad (2)$$

where $\delta\mathbf{S}^L$ is the virtual stress vector.

The stress vector $\mathbf{S}^L$ and the strain vector $\mathbf{E}^L$ are related as

$$\mathbf{S}^L = \mathbf{C}_e \mathbf{E}^L, \qquad (3)$$

where $\mathbf{C}_e$ is the 6×6 elastic constant matrix defined in the local coordinate system. The virtual stress vector $\delta\mathbf{S}^L$ in eqn (2) is related to the virtual strain vector $\delta\mathbf{E}^L$ as follows:

$$\delta\mathbf{S}^L = \mathbf{C}_e \delta\mathbf{E}^L. \qquad (4)$$

Using eqns (3) and (4), the equilibrium equation and the compatibility condition can be expressed as

$$\int (\delta\bar{\mathbf{E}}^L)^T \mathbf{C}_e \mathbf{E}^L \,\mathrm{d}v - \delta W = 0 \qquad (5)$$

$$\int (\delta\mathbf{E}^L)^T \mathbf{C}_e (\bar{\mathbf{E}}^L - \mathbf{E}^L)\,\mathrm{d}v = 0. \qquad (6)$$

For thin shells, the strain components can be assumed to be linear in the thickness direction. Then the displacement-dependent strain vectors $\bar{\mathbf{E}}^L$ can be expressed symbolically as

$$\bar{\mathbf{E}}^L = \bar{\mathbf{E}}_0 + \zeta\bar{\mathbf{E}}_\zeta, \qquad (7a)$$

where $\zeta(-1 \le \zeta \le 1)$ is the parent coordinate in the thickness direction. In the above equations, $\bar{\mathbf{E}}_0$ and $\bar{\mathbf{E}}_\zeta$ are independent of ζ and can be expressed as follows:

$$\bar{\mathbf{E}}_0 = \frac{1}{2}(\bar{\mathbf{E}}^L_a + \bar{\mathbf{E}}^L_{-a}) \qquad (7b)$$

$$\bar{\mathbf{E}}_\zeta = \frac{1}{2a}(\bar{\mathbf{E}}^L_a - \bar{\mathbf{E}}^L_{-a}), \qquad (7c)$$

where $\bar{\mathbf{E}}^L$ with subscript a or $-a$ indicates that it is evaluated at $\zeta = a$ or $\zeta = -a$. In this study, $a = \frac{1}{\sqrt{3}}$, corresponding to the two point Gaussian integration rule. Similarly

$$\delta\bar{\mathbf{E}}^L = \delta\bar{\mathbf{E}}_0 + \zeta\delta\bar{\mathbf{E}}_\zeta \qquad (8a)$$

$$\mathbf{E}^L = \mathbf{E}_0 + \zeta\mathbf{E}_\zeta \qquad (8b)$$

$$\delta\mathbf{E}^L = \delta\mathbf{E}_0 + \zeta\delta\mathbf{E}_\zeta, \qquad (8c)$$

where all the vector quantities in the right hand side are independent of ζ.

The determinant J of the Jacobian matrix is also assumed to be linear in thickness direction and can be expressed as

$$J = J_0 + \zeta J_\zeta = (1 + r\zeta)J_0, \qquad (9)$$

where J_0 and J_ζ are determined from J evaluated at $\zeta = a$ and $\xi = -a$, and $r = J_\zeta/J_0$.

Using eqns (7a), (8a)–(8c) and (9), eqns (5) and (6) can be integrated analytically in the ζ direction such that

$$\sum_e \left[\int \delta\bar{\mathbf{E}}^T \mathbf{C}\mathbf{E}\,\mathrm{d}A_e - \delta W_e\right] = 0 \qquad (10)$$

$$\sum_e \int \delta\mathbf{E}^T \mathbf{C}(\bar{\mathbf{E}} - \mathbf{E})\,\mathrm{d}A_e = 0, \qquad (11)$$

where the notation Σ with subscript e stands for summation over elements and the variables with subscript e indicate the elemental quantities, and

$$\bar{\mathbf{E}} = \begin{Bmatrix}\bar{\mathbf{E}}_0\\ \bar{\mathbf{E}}_\zeta\end{Bmatrix} \qquad (12a)$$

$$\mathbf{E} = \begin{Bmatrix}\mathbf{E}_0\\ \mathbf{E}_\zeta\end{Bmatrix} \qquad (12b)$$

$$\delta\bar{\mathbf{E}} = \begin{Bmatrix}\delta\bar{\mathbf{E}}_0\\ \delta\bar{\mathbf{E}}_\zeta\end{Bmatrix} \qquad (12c)$$

$$\delta\mathbf{E} = \begin{Bmatrix}\delta\mathbf{E}_0\\ \delta\mathbf{E}_\zeta\end{Bmatrix} \qquad (12d)$$

$$\mathrm{d}A_e = J_0\,\mathrm{d}\xi\,\mathrm{d}\eta. \qquad (12e)$$

In the above equations, the integrated elastic constant matrix $\mathbf{C}$ is defined as

$$\mathbf{C} = \begin{bmatrix}\mathbf{C}_1 & \mathbf{C}_2\\ \mathbf{C}_2 & \mathbf{C}_3\end{bmatrix}, \qquad (13)$$

where

$$\mathbf{C}_1 = \int \mathbf{C}_e\,\mathrm{d}\zeta + r\int \zeta\mathbf{C}_e\,\mathrm{d}\zeta \qquad (14a)$$

$$\mathbf{C}_2 = \int \zeta \mathbf{C}_e \, d\zeta + r \int \zeta^2 \mathbf{C}_e \, d\zeta \tag{14b}$$

$$\mathbf{C}_3 = \int \zeta^2 \mathbf{C}_e \, d\zeta + r \int \zeta^3 \mathbf{C}_e \, d\zeta. \tag{14c}$$

For laminated composite shells, the above integrations in ζ are carried out analytically.

In accordance with the Newton–Raphson method, incremental quantities are introduced for the displacement-dependent strain vector as follows:

$$\bar{\mathbf{E}} = {}^k\bar{\mathbf{E}} + \Delta\bar{\mathbf{e}} + \Delta\bar{\mathbf{n}}, \tag{15}$$

where ${}^k\bar{\mathbf{E}}$ represents the resulting strain vector of the kth iteration; $\Delta\bar{\mathbf{e}}$ and $\Delta\bar{\mathbf{n}}$ are linear and nonlinear in incremental displacement.

The virtual strain vector $\delta\bar{\mathbf{E}}$ can be expressed symbolically as

$$\delta\bar{\mathbf{E}} = \delta\bar{\mathbf{e}} + \delta\bar{\mathbf{n}}, \tag{16}$$

where $\delta\bar{\mathbf{e}}$ is independent of the incremental displacement and $\delta\bar{\mathbf{n}}$ is linear in incremental displacement.

In addition, the independent strain vector is expressed in incremental form as follows:

$$\mathbf{E} = {}^k\mathbf{E} + \Delta\mathbf{e}. \tag{17}$$

Using eqns (15), (16) and (17) and neglecting higher order terms, eqns (10) and (11) can be rewritten as

$$\sum_e \int [\delta\bar{\mathbf{e}}^T \mathbf{C} \Delta\mathbf{e} + \delta\bar{\mathbf{n}}^T \mathbf{C}\,{}^k\mathbf{E} + \delta\bar{\mathbf{e}}^T \mathbf{C}\,{}^k\mathbf{E}] \, dA_e - \sum_e \delta W_e = 0 \tag{18}$$

$$\sum_e \int \delta\mathbf{E}^T \mathbf{C}({}^k\bar{\mathbf{E}} - {}^k\mathbf{E}) \, dA_e + \sum_e \int \delta\mathbf{E}^T \mathbf{C}(\Delta\bar{\mathbf{e}} - \Delta\mathbf{e}) \, dA_e = 0. \tag{19}$$

The incremental strain vector can be expressed as

$$\Delta\bar{\mathbf{e}} = \mathbf{B}\Delta\mathbf{q}_e, \tag{20}$$

where the $\mathbf{B}(\xi, \eta)$ matrix relates the incremental strain to the incremental nodal displacement vector $\Delta\mathbf{q}_e$. Similarly, for the virtual strain vector

$$\delta\bar{\mathbf{e}} = \mathbf{B}\delta\mathbf{q}_e, \tag{21}$$

where $\delta\mathbf{q}_e$ is the virtual nodal displacement vector.

Meanwhile, the assumed incremental strain vector $\Delta\mathbf{e}$ and the virtual stratin vector $\delta\mathbf{E}$ can be expressed as

$$\Delta\mathbf{e} = \mathbf{P}\mathbf{b} \tag{22a}$$

$$\delta\mathbf{E} = \mathbf{P}\delta\mathbf{b}, \tag{22b}$$

where $\mathbf{P}(\xi, \eta)$ is the assumed strain shape function matrix and $\mathbf{b}$ is the strain parameter vector.

Introducing eqns (20), (22a) and (22b), eqn (19) for compatibility condition can be written as follows:

$$\sum_e \delta\mathbf{b}^T(\mathbf{G}\Delta\mathbf{q}_e - \mathbf{H}\mathbf{b} + \mathbf{F}) = 0, \tag{23}$$

where

$$\mathbf{F} = \int \mathbf{P}^T \mathbf{C}({}^k\bar{\mathbf{E}} - {}^k\mathbf{E}) \, dA_e \tag{24a}$$

$$\mathbf{G} = \int \mathbf{P}^T \mathbf{C}\mathbf{B} \, dA_e \tag{24b}$$

$$\mathbf{H} = \int \mathbf{P}^T \mathbf{C}\mathbf{P} \, dA_e. \tag{24c}$$

From eqn (23)

$$\mathbf{G}\Delta\mathbf{q}_e - \mathbf{H}\mathbf{b} + \mathbf{F} = 0 \tag{25a}$$

for each element or

$$\mathbf{b} = \mathbf{H}^{-1}\mathbf{G}\Delta\mathbf{q}_e + \mathbf{H}^{-1}\mathbf{F}, \tag{25b}$$

which is the discretized compatibility condition at element level.

Using eqns (21) and (22a), eqn (18) for linearized equilibrium becomes

$$\sum_e \delta\mathbf{q}_e^T(\mathbf{G}^T\mathbf{b} + \mathbf{K}_S\Delta\mathbf{q}_e + {}^k\mathbf{Q} - \mathbf{Q}_a) = 0, \tag{26}$$

where $\mathbf{K}_S$ is the initial stress stiffness matrix and

$${}^k\mathbf{Q} = \int \mathbf{B}^T \mathbf{C}\,{}^k\mathbf{E} \, dA_e \tag{27}$$

and the external load vector $\mathbf{Q}_a$ is defined as

$$\delta W_e = \delta\mathbf{q}_e^T \mathbf{Q}_a. \tag{28}$$

Using eqns (25b), eqn (26) can be rewritten as

$$\sum_e \delta\mathbf{q}_e^T[\mathbf{G}^T\mathbf{H}^{-1}(\mathbf{G}\Delta\mathbf{q}_e + \mathbf{F}) + \mathbf{K}_S\Delta\mathbf{q}_e + {}^k\mathbf{Q} - \mathbf{Q}_a] = \sum_e \delta\mathbf{q}_e^T[\mathbf{K}_e\Delta\mathbf{q}_e - \Delta\mathbf{Q}_e] = 0, \tag{29}$$

where

$$\mathbf{K}_e = \mathbf{G}^T\mathbf{H}^{-1}\mathbf{G} + \mathbf{K}_S \tag{30a}$$

$$\Delta\mathbf{Q}_e = \mathbf{Q}_a - \mathbf{G}^T\mathbf{H}^{-1}\mathbf{F} - {}^k\mathbf{Q}. \tag{30b}$$

After assembling over all elements, eqn (29) becomes

$$\delta \mathbf{q}^T(\mathbf{K}\Delta\mathbf{q} - \Delta\mathbf{Q}) = 0, \tag{31}$$

where $\mathbf{K}$ is the global tangent stiffness matrix, $\Delta\mathbf{q}$ is the global incremental nodal displacement vector and $\Delta\mathbf{Q}$ is the global incremental nodal load vector. From eqn (31)

$$\mathbf{K}\Delta\mathbf{q} = \Delta\mathbf{Q}, \tag{32}$$

which can be solved for $\Delta\mathbf{q}$.

Assumed strain

The choice of assumed strain is very critical for the performance of finite element model. In [9] various sets of assumed strain were tested to check the performance of the 18-node solid element model. The assumed strain field used in the present paper is based on the study conducted in [9]. For the convenience of discussion, the assumed strain vector is expressed as the sum of the lower order assumed strain vector $\Delta\mathbf{e}^L$ and higher order assumed strain vector $\Delta\mathbf{e}^H$ as follows:

$$\Delta\mathbf{e} = \Delta\mathbf{e}^L + \Delta\mathbf{e}^H. \tag{33}$$

In the above equation every component of lower order strain vector $\Delta\mathbf{e}^L$ is assumed to be bilinear in ξ and η except $(\Delta e_{zz})^L_\zeta$. For example,

$$\begin{aligned}(\Delta e_{xx})^L_0 &= b_1 + b_2\xi + b_3\eta + b_4\xi\eta \\ &\cdots\cdots\cdots\cdots\cdots\cdots \\ (\Delta e_{xx})^L_\zeta &= b_{41} + b_{42}\xi + b_{43}\eta + b_{44}\xi\eta.\end{aligned} \tag{34a}$$

However,

$$(\Delta e_{zz})^L_\zeta = 0. \tag{34b}$$

On the other hand, the higher order strain field is chosen as follows:

$$\begin{aligned}(\Delta e_{xx})^H_0 &= \xi\eta^2 b_{45} \\ (\Delta e_{yy})^H_0 &= \xi^2\eta b_{46} \\ (\Delta e_{zz})^H_0 &= (\Delta e_{xy})^H_0 = 0 \\ (\Delta e_{yz})^H_0 &= \xi^2\eta b_{47} \\ (\Delta e_{zx})^H_0 &= \xi\eta^2 b_{47} \\ (\Delta e_{xx})^H_\zeta &= \xi\eta^2 b_{48} \\ (\Delta e_{yy})^H_\zeta &= \xi^2\eta b_{49} \\ (\Delta e_{zz})^H_\zeta &= (\Delta e_{xy})^H_\zeta = 0 \\ (\Delta e_{yz})^H_\zeta &= \xi^2\eta b_{50} \\ (\Delta e_{zx})^H_\zeta &= \xi\eta^2 b_{50}.\end{aligned} \tag{35}$$

As demonstrated in [9], the above assumed strain field in conjunction with the 3×3 point integration rule results in a finite element model which is free of locking while kinematically stable when elements are assembled.

Modified stress–strain relation

The stress–strain relation for a three dimensional solid can be modified to model the behavior of thin shell structure by ignoring the effect of normal stress S_{zz} on strain components E_{xx} and E_{yy}. For transversely isotropic laminated composite shells, the modified stress–strain relations in the local coordinate system are as follows:

$$\begin{aligned}E_{xx} &= A_{11}S_{xx} + A_{12}S_{yy} + A_{14}S_{xy} \\ E_{yy} &= A_{21}S_{xx} + A_{22}S_{yy} + A_{24}S_{xy} \\ E_{zz} &= A_{33}S_{zz} \\ E_{xy} &= A_{41}S_{xx} + A_{42}S_{yy} + A_{44}S_{xy} \\ E_{yz} &= A_{55}S_{yz} + A_{56}S_{zx} \\ E_{zx} &= A_{65}S_{yz} + A_{66}S_{zx},\end{aligned} \tag{36}$$

where A_{ij} are the compliance coefficients in local coordinate system. The modified elastic coefficient matrix $\mathbf{C}_e$ is determined by inverting the relationship in eqn (36).

3. NUMERICAL TEST

Two simple numerical tests with geometrically nonlinear laminated composite plates and shells were performed in order to check the validity and the accuracy of the present approach. In the finite element modelling, only one element is used in the thickness direction.

(a) Square plate

Figure 2 shows a clamped composite square plate under uniformly distributed load. The

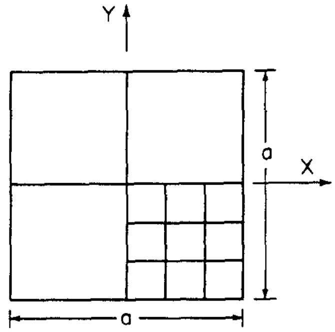

Fig. 2. Square plate (3×3 element mesh for a quarter plate).

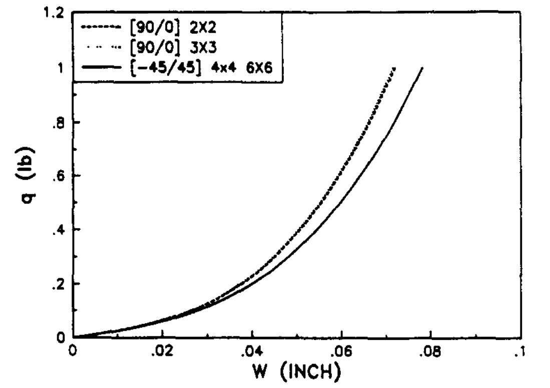

Fig. 3. Vertical displacement of square plate under uniform loading.

dimensions of the square plate are $a = 9$ in. and thickness $t = 0.04$ in. Elastic properties are Young's moduli $E_1 = 20 \times 10^6$ psi, $E_2 = 1.4 \times 10^6$ psi, shear moduli $G_{12} = G_{23} = G_{31} = 0.7 \times 10^6$ psi and Poisson's ratios $\nu_{12} = \nu_{23} = \nu_{31} = 0.3$. Two layups, [90/0°] and [−45/45°] were tested. For the cross-ply laminate with [90/0°] layup, only a quarter of the square plate is modelled with 2×2 and 3×3 mesh over the X–Y plane because of the symmetry in loading and geometry. However, for the angle-ply laminate with [−45/45°] layup, the entire plate is modelled with 4×4 and 6×6 mesh. Figure 3 shows the vertical deflection at the center of the plate under increasing pressure for the cross-ply and the angle-ply laminates. In the figure the results show good convergence characteristics. Particularly for the angle-ply case, the results with 4×4 and 6×6 mesh are almost equal to each other. Figure 4 shows the vertical deflection along the X axis under uniform pressure $q = 1$ psi. For the cross-ply laminate, the present results agree well with those reported in [5].

(b) *Cylindrical shell*

Figure 5 shows a [0/90°] composite cylindrical shell under uniformly distributed load. All boundaries are clamped and the dimensions are $R = 2540$ in., $L = 508$ in., $t = 2.54$ in. and $\theta = 0.2$ rad.

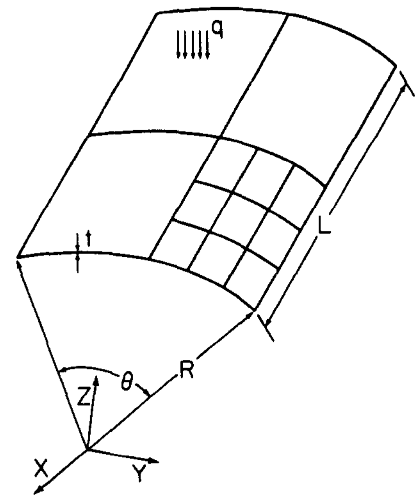

Fig. 5. Cylindrical shell (3×3 element mesh for a quarter of the shell).

Elastic properties are $E_1 = 25 \times 10^6$ psi, $E_2 = 10^6$ psi, $G_{12} = G_{31} = 0.5 \times 10^6$ psi, $G_{23} = 0.2 \times 10^6$ psi and $\nu_{12} = \nu_{23} = \nu_{31} = 0.25$. Because of the symmetry of the structure, only a quarter of the cylindrical shell was modelled with 3×3 and 4×4 mesh. Figure 6 shows the vertical deflections at the center of the shell under increasing uniform pressure. The results show good convergence characteristics. As shown in the figure, the present approach shows substantially different responses from those reported in [10] as the pressure increases. The discrepancy may be due to the differences in mesh size or element modelling. For example, [10] does not report any convergence test.

4. CONCLUSION

The results of numerical tests demonstrate the validity and the accuracy of the present approach in modelling the geometrically nonlinear behavior of composite thin shell structures. The linear assumption of strain and the determinant of the Jacobian matrix allows analytical integration in the thickness direction for composite thin shells. Al-

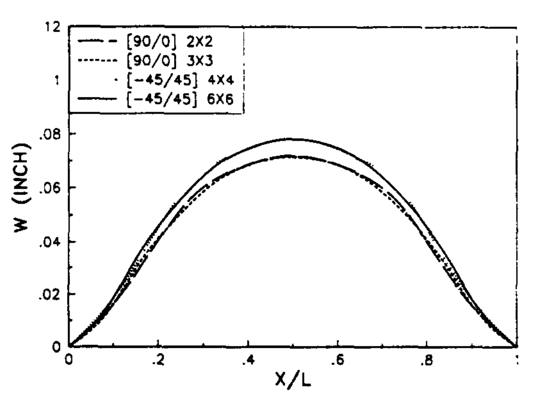

Fig. 4. Vertical displacement of square plate along X axis ($q = -1.0$ psi).

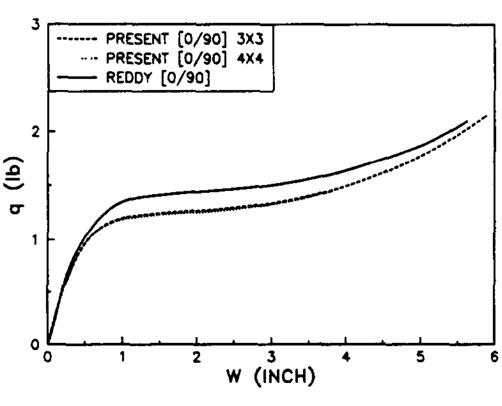

Fig. 6. Vertical displacement of cylindrical shell under uniform load.

though only simple examples were considered in the numerical test, it is clear that the present approach is capable of modelling composite thin shells of arbitrary geometry. With minor modification, the present formulation can handle more complex problems such as the delamination buckling of composite structures.

Acknowledgement—The present work has been supported by the ONR and the University of Illinois at Urbana-Champaign through the ONR-URI program. The bulk of computing time has been provided by the Computer Science Center at the University of Maryland.

REFERENCES

1. A. K. Noor and S. J. Hartley, Nonlinear shell analysis via mixed isoparametric elements. *Comput. Struct.* **7**, 615–626 (1977).
2. J. N. Reddy, Bending of laminated anisotropic shells by a shear deformable finite element. *Fibre Sci. Technol.* **17**, 9–24 (1982).
3. S. Saigal, R. K. Kapania and T. Y. Yang, Geometrically nonlinear finite element analysis of imperfect laminated shells. *J. Comp. Mater.* **20**, 197–214 (1986).
4. T. Y. Chang and K. Sawamiphakdi, Large deformation analysis of laminated shells by finite element method. *Comput. Struct.* **13**, 331–340 (1981).
5. C. H. Yeom and S. W. Lee, An assumed strain finite element model for large deflection composite shells. In *Proceedings of AIAA/ASME/ASCE/AHS 29th Structures, Structural Dynamics and Materials Conference*, Part 2, pp. 928–936. Williamsburg, VA (1988).
6. S. W. Lee and T. H. H. Pian, Improvement of plate and shell finite element by mixed formulations. *AIAA Jnl* **16**, 29–34 (1978).
7. J. J. Rhiu and S. W. Lee, A new efficient mixed formulation for thin shell finite element models. *Int. J. Numer. Meth. Engng.* **24**, 581–604 (1987).
8. M. F. Ausserer and S. W. Lee, An eighteen node solid element for thin shell analysis. *Int. J. Numer. Meth. Engng* **26**, 1345–1364 (1988).
9. Y. H. Kim and S. W. Lee, Finite element analysis of shell structures with a solid element. Internal Report, Department of Aerospace Engineering, University of Maryland, MD (1988).
10. J. N. Reddy and K. Chandrashekhara, Nonlinear analysis of laminated shells including transverse shear strains. *AIAA Jnl* **23**, 440–441 (1985).